Drug Design, Development and Therapy

Dovepress
open access to scientific and medical research

Open Access Full Text Article

ORIGINAL RESEARCH

Benzoylaconine Protects Skeletal Muscle Against Ischemia-Reperfusion Injury Through Activation of IF1-Dependent AMPK/Nrf2 Axis

Yidong Cui[1], Qingming Liu[2], Qiqiang Zhang[3], Xuemei Di[3], Hai Zhang[3]

[1]Department of Orthopedic Surgery, The First Affiliated Hospital of Shandong First Medical University & Shandong Provincial Qianfoshan Hospital, Jinan, 250014, People's Republic of China; [2]Department of Neurology, Shandong Second Provincial General Hospital, Jinan, 250012, People's Republic of China; [3]Department of Pharmacy, Shanghai First Maternity and Infant Hospital, School of Medicine, Tongji University, Shanghai, 200092, People's Republic of China

Correspondence: Hai Zhang, Department of Pharmacy, Shanghai First Maternity and Infant Hospital, School of Medicine, Tongji University, No. 2699 West Gaoke Road, Shanghai, 200092, People's Republic of China, Tel/Fax +8621-20261401, Email zhxdks2005@126.com

Background: *Aconitum carmichaelii* (Fuzi) has been conventionally used to cure a variety of ailments, such as pain, cold sensations, and numbness of limb muscles (Bi Zheng) in China. Our prior investigations identified Benzoylaconine (BAC) as a bioactive alkaloid derived from *Aconitum carmichaelii*, with other studies also demonstrating its significant pharmacological potential.

Purpose: This study aimed to explore the potential of BAC as a protective agent against skeletal muscle ischemia-reperfusion (I/R) injury and to elucidate the underlying mechanisms.

Methods: In vivo models involved subjecting Sprague-Dawley rats to I/R through femoral artery ligation followed by reperfusion, while in vitro models utilized C2C12 cells subjected to hypoxia/reoxygenation (H/R). CCK-8 assay was used to assess cell viability. TUNEL staining and flow cytometric analysis were used to measure cell apoptosis. Biochemical assay was used to assess skeletal muscle injury and oxidative stress. Immunofluorescence and Western blot were performed to determine protein levels.

Results: BAC effectively protected muscle tissue from I/R injury, enhancing cell viability ($p<0.01$), elevating SOD levels ($p<0.05$), and reducing CK ($p<0.01$), LDH ($p<0.01$), ROS ($p<0.01$), MDA ($p<0.01$), and apoptosis-related molecules in vivo and in vitro ($p<0.05$, $p<0.01$). Mechanistically, BAC increased the expression of IF1, phosphorylated AMPK, facilitated the translocation of nuclear Nrf2, and induced the expression of HO-1 ($p<0.01$). Notably, AMPK inhibitor Compound C significantly hindered the ability of BAC to ameliorate H/R-induced cell injury ($p<0.05$), oxidative stress($p<0.01$), and apoptosis ($p<0.05$), as well as promote Nrf2 nuclear translocation ($p<0.01$). Moreover, silencing of IF1 with siRNA abolished BAC-induced activation of AMPK/Nrf2 axis ($p<0.01$).

Conclusion: Our study provides novel evidence supporting the potential of BAC as a myocyte-protective agent against I/R injury, and we establish a previously unknown mechanism involving the activation of the IF1-dependent AMPK/Nrf2 axis in mediating the protective effects of BAC.

Keywords: Benzoylaconine, ischemia-reperfusion injury, oxidative stress, AMPK, IF1

Introduction

Skeletal muscle ischemia-reperfusion (I/R) injury poses a significant clinical challenge and can lead to severe complications. It is associated with various conditions such as crush syndrome, compartment syndrome, vascular injury, and surgical procedures.[1,2] Compared to other tissues, skeletal muscle is particularly vulnerable to the damaging effects of I/R due to its limited regenerative capacity and the formation of fibrosis and scar tissue.[3] The detrimental consequences of I/R injury include loss of muscle function, limb amputation, and even systemic organ dysfunction.[4] Despite previous studies on potential treatments, there is still a lack of effective clinical therapies.[5] Therefore, understanding the mechanisms underlying I/R injury and developing novel therapeutic approaches are crucial for improving patient outcomes.

The processed lateral root of *Aconitum carmichaelii* Debeaux (Ranunculaceae), commonly known as "Fuzi", has been officially documented in the Chinese pharmacopoeia with an extended history of usage in traditional Chinese medicine.[6]

Received: 26 December 2023
Accepted: 7 June 2024
Published: 10 June 2024

Graphical Abstract

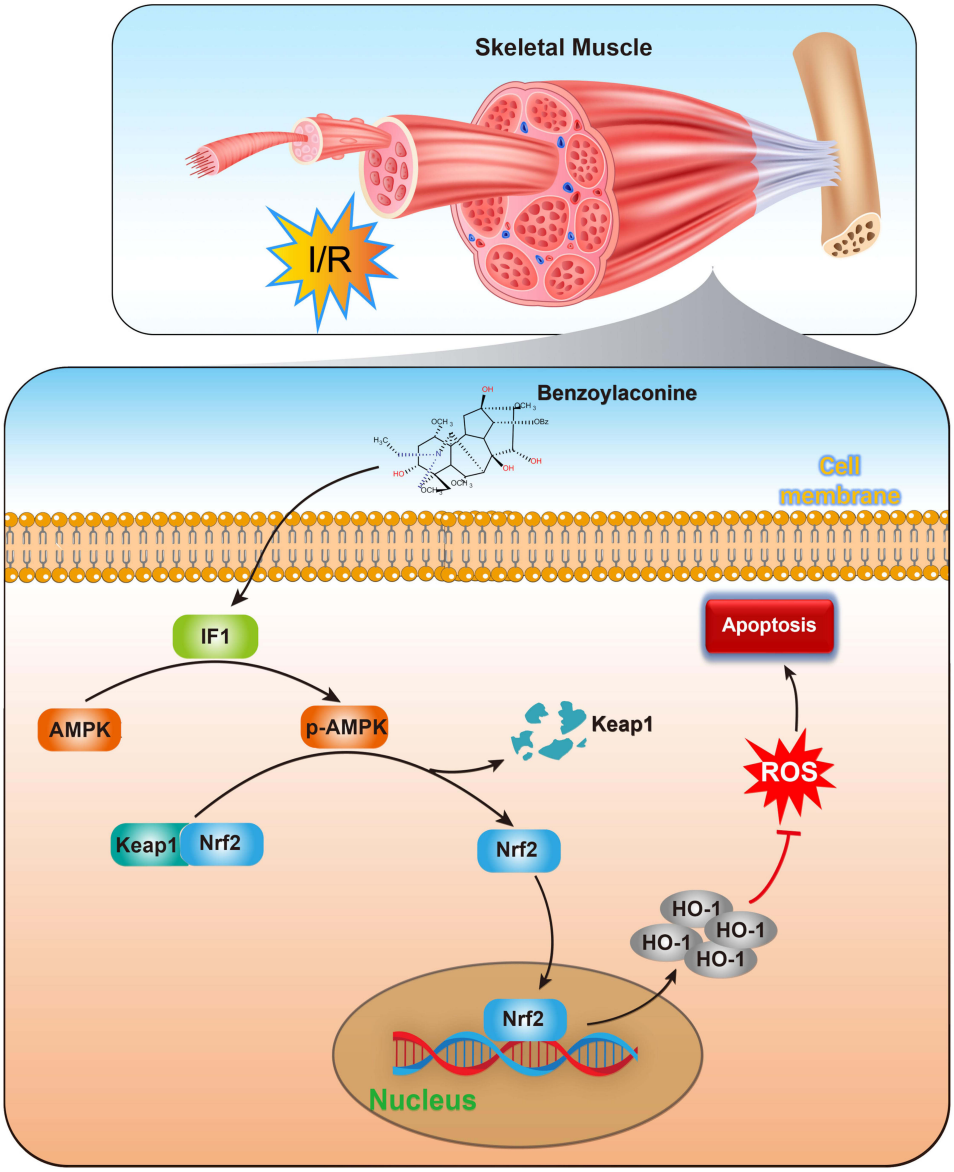

Its traditional applications include treating cardiovascular diseases and relieving pain, cold, and numbness of limb muscles (Bi Zheng). The alkaloids present in *Aconitum carmichaelii* Debeaux are considered to be the most predominant active ingredients. In our previous studies, we conducted a screening of bioactive alkaloids in *Aconitum carmichaelii* Debeaux and found that benzoylaconine (BAC) exhibited significant anti-hypertensive and anti-heart failure effects.[6,7] Additionally, other scholars have demonstrated the significant pharmacological potential of BAC, including analgesic, anti-inflammatory, and anti-tumor properties.[8,9] Furthermore, our systematic analysis revealed that BAC is the main monoester-diterpenoid alkaloid after boiling and metabolism.[10,11] Notably, BAC demonstrated a low T_{max} value and high $t_{1/2}$, indicating rapid absorption and slow metabolism or excretion.[12,13] Additionally, other scholars have found that BAC has a relatively high safety profile, having 1500 mg kg^{-1} oral median lethal dosage (LD50) in mice.[14] Based on these findings, we hypothesized that BAC presents potential therapeutic benefits for skeletal muscle ischemia-reperfusion injury.

The stress response kinase known as adenosine monophosphate (AMP)-activated protein kinase (AMPK) is of significant importance in the regulation of several physiological and metabolic processes. These activities include but are not limited to cell apoptosis, energy balance, and cell metabolism.[15–17] The AMPK has the ability to augment cellular antioxidant enzyme systems, hence reducing oxidative damage in the I/R injury.[18] Due to its crucial role in regulating stress and cellular energy balance, AMPK has garnered significant interest as a potential treatment option for several human diseases.[19] The process of phosphorylating AMPK triggers the commencement of nuclear factor erythroid 2-related factor 2 (Nrf2) activation, which has a crucial role in controlling antioxidant activity. This activation subsequently results in the decrease of free radicals through the upregulation of heme oxygenase 1 (HO-1), which is one of the downstream effectors regulated by Nrf2. Numerous studies have repeatedly shown the significant importance of Nrf2 as a downstream target of AMPK signaling in bestowing resistance against inflammatory responses and oxidative damage.[20,21] The signaling pathway of AMPK/Nrf2 safeguards cells from reactive oxygen species (ROS) and inflammatory damage by initiating antioxidant cascades.[22,23] Interestingly, BAC has been reported to activate AMPK under oxidative stress conditions.[9]

AMPK activity is tightly regulated by ATP levels. One crucial protein involved in this process is ATPase inhibitory factor 1 (IF1), which interacts with F1F0-ATP synthase.[24,25] The reversal of F1F0-ATP synthase's function, leading to ATP hydrolysis, is followed by the attachment of IF1 to the ATP synthase, therefore inhibiting its activity. Consequently, this inhibition causes a notable reduction in the inner membrane potential.[26] Therefore, the IF1 protein assumes a crucial function in safeguarding against the depletion of overall ATP and consequent cell death in situations of hypoxia or nutrient deprivation, thereby underscoring its indispensable involvement in pathological circumstances.[27] Recent research has elucidated the regulatory function of IF1 in the activity of AMPK and its subsequent molecular pathways.[25,26]

In this study, our objective was to explore the effects of BAC on I/R injury in skeletal muscle, as well as its underlying mechanism. Building upon the previously mentioned observations, our hypothesis posits that BAC exerts a protective influence on skeletal muscle injury by upregulating IF1 expression, enhancing AMPK phosphorylation, facilitating Nrf2 nuclear translocation, and increasing HO-1 expression. Ultimately, these actions contribute to the inhibition of oxidative damage and apoptosis in myocytes.

Materials and Methods

Experimental Animals

Sprague-Dawley (SD) rats (male; weight = 200–250 g; age = 6 and 8 weeks) were obtained from Charles River Co., Ltd. (Beijing, China). The rats were allowed to adapt to a controlled environment (temperature = 18–25°C; humidity = 55 ± 5%; normal light/dark cycle) for 1 week. The ethics committee of the Tongji University School of Medicine (Shanghai, China, NO. TJBG00122101) granted approval for the protocols employed in this study. Additionally, the Shanghai First Maternity and Infant Hospital, Tongji University School of Medicine (Shanghai, 201,204, China) provided authorization, ensuring compliance with the ethical guidelines set forth by the National Institute of Health regarding the usage of experimental animals.

Experimental Groups and Drug Treatment

Benzoylaconine (BAC, purity, HPLC ≥ 98%, No: ST21850120-20mg, CAS#466-24-0, molecular formula: C32H45NO10, molecular weight: 603.70), and N-acetylcysteine (NAC, purity, HPLC ≥ 98%, No: ST84670120-20mg, CAS#616-91-1, molecular formula: C5H9NO3S, molecular weight: 163.19) were procured from Nature-Standard Co., Ltd. (Shanghai, China). The chemical structure of Benzoylaconine is shown in the Graphical abstract. In this study, six groups of six rats, each formed by random selection out of a total of thirty-six rats. Following the injection of a 3% pentobarbital solution for anesthesia (50 mg/kg, intraperitoneally), the femoral artery of the right hind limb was exposed, and blood flow was halted using a non-traumatic microvascular clamp. Additionally, an elastic tourniquet was placed on the trochanteric region of the femur to prevent collateral circulation. The ischemia was identified by the lack of arterial pulse, cyanosis, and coldness of the limb. According to previous studies,[4] all experimental animals in the study were subjected to a standardized procedure involving 3 h of ischemia followed by 24 h of reperfusion, with the exception of the sham group. The femoral artery was surgically exposed for a duration of 3 h in the sham group without any further operations, and the rats were administered intraperitoneal injection of saline prior to reperfusion. Based on our previous

study, we chose the dose of 5 mg/kg, 10 mg/kg, and 20 mg/kg for BAC.[6] The femoral artery was occluded for 3 h in the I/R + BAC 5 mg/kg, 10 mg/kg, and 20 mg/kg groups, and the rats received intraperitoneal injections of saline containing BAC at 5, 10, and 20 mg/kg, respectively, before reperfusion. Following 3 h of femoral artery blockage, rats were intraperitoneally administered with 10 mg/kg NAC-containing saline before reperfusion in the I/R+NAC group. To collect skeletal muscle tissue samples (including gastrocnemius and tibialis anterior), the mice were anesthetized using an intraperitoneal injection of an overdose of 3% pentobarbital (135 mg/kg). Skeletal muscle tissue was collected and divided into different sections for various tests.

Wet Weight/Dry Weight Ratio (W/D) of Muscle Tissue

The tibialis anterior muscle was expeditiously weighed upon removal from the right hind leg of each rat, measuring its wet weight. Following this, the samples underwent dehydration and were subsequently reweighed to determine their dry weight. In order to evaluate the presence of tissue edema, the wet-to-dry ratio was calculated utilizing the following formula: wet/dry ratio = (wet weight/dry weight) × 100%.[4,28]

Hematoxylin-Eosin (H&E) Staining

The specimens of skeletal muscle were fixed by submerging them in a solution containing 10% paraformaldehyde. Subsequently, the paraffin-embedded samples were sliced into thin sections measuring 5 μm in thickness. Afterward, the sections were mounted onto slides for performing H&E staining. The slides were analyzed using an optical microscope (BH-Z; Olympus Corporation, Japan). The histological damage scores were determined following a methodology from a prior study.[29] Briefly, Five fields of the sections were randomly selected for assessment at ×400 magnification. Three blinded observers scored morphological impairment based on muscle fiber disorganization, degeneration, and neutrophil infiltration. Each criterion was graded on a scale ranging from 0 (normal findings) to 3 (very distinctive findings).

TUNEL Staining

In order to assess apoptotic cells in skeletal muscle, a TUNEL assay was performed. The DNA Fragmentation Detection Kit (Millipore, QIA39-1EA) was employed in accordance with the prescribed instructions. The muscle slices fixed in paraffin were first subjected to deparaffinization and permeabilization using a solution of 20 μg/mL proteinase K in 10 mM Tris-HCl for a duration of 15 minutes. Following that, blocking was done using 10% normal goat serum in phosphate-buffered saline (PBS) at ambient temperature for a duration of 60 minutes. Utilizing a confocal microscope (Eclipse TI, Nikon, Tokyo, Japan), images of the stained sections were captured. The 4',6-diamidino-2-phenylindole (DAPI) dye was utilized to achieve blue staining of the nuclei, while the apoptotic cells were distinguished as green as a result of TUNEL positivity. A cell count was performed to quantify the number of cells positive for both TUNEL and DAPI staining. The percentage of TUNEL-positive cells was computed by green/blue * 100%.

Cell Culture and Hypoxia/Reoxygenation (H/R) Model

The C2C12 myoblasts were cultivated in DMEM containing FBS (10%) in standard incubation conditions. The myoblasts were stimulated to differentiate by treatment with 2% horse serum for a duration of 6 days. The hypoxia/reoxygenation (H/R) model was generated by subjecting the cells to hypoxic conditions. For this cells were incubated in DMEM devoid of serum and glucose for a duration of 5 h. The hypoxic conditions consisted of an atmosphere containing 94% nitrogen, 1% oxygen, and 5% carbon dioxide. Following this, the cells were reintroduced to a standard DMEM media and placed in a normoxic environmental condition for a period of 2 h.

Cell Transfection

The custom design and synthesis of negative control siRNA and IF1 siRNA sequences were prepared by Sangon (Shanghai, China). The transfection of siRNA was conducted in C2C12 cells that were cultivated in 6-well plates, utilizing Lipofectamine RNAiMAX as the transfection reagent. The efficacy of siRNA-mediated interference was evaluated through Western blotting (WB) analysis.

Cell Treatments

The cell experiment comprised three distinct sections. In the initial phase, the cells were placed into six groups at random: (A) Control, the C2C12 cells were cultivated using standard procedures for a duration of 7 h; (B) H/R, the cells were subjected to a 5-h hypoxic phase and a 2-h reoxygenation period following that; (C-E) H/R + BAC (20 μM-60 μM), the cells underwent pre-treatment with varying concentrations of BAC (20 μM-60 μM) for a duration of 1 h before H/R; (F) H/R + NAC (Positive control), the cells had an hour of pre-treatment with a 20 μM dose of NAC before the H/R. In the second phase, the cells were randomly allocated into four distinct groups: (A) Control; (B) H/R; (C) H/R + BAC, before H/R, the cells underwent pre-treatment with 60 μM of BAC for 1 h; (D) H/R + BAC + CC, the cells were subjected to a 24 h treatment with a concentration of 10 μM Compound C, followed by a further 1 h treatment with a concentration of 60 μM BAC before the initiation of H/R. In the third phase, a random division of the cells was done into five distinct groups: (A) Control; (B) H/R; (C) H/R + BAC; (D) H/R + BAC + SiIF1-NC, the cells were transfected with scramble negative control siRNAs (si-NC) and, after that, exposed to a 60 μM concentration of BAC for a duration of 1 h prior to H/R; (E) H/R+BAC+SiIF1, the cells were transfected with IF1 siRNA and then exposed to a 60 μM concentration of BAC for a duration of 1 h prior to H/R.

Cell Viability Assay

The cell viability was assessed using a CCK-8 kit (Beyotime Biotech, Shanghai, China). Concisely, 5000 C2C12 cells/well were seeded in 96-well plate, followed by an overnight incubation. After the completion of the respective treatments, 10 μL/well of CCK-8 solution was introduced and incubated for an additional 1 h. The measurement of absorbance was conducted at a wavelength of 450 nm using a microplate reader (Synergy H1, BioTek, USA).

Skeletal Muscle Damage Assessment Serum

A clinical autoanalyzer (7600–020; Hitachi, Tokyo, Japan) was used to evaluate the levels of lactate dehydrogenase (LDH) and creatine kinase (CK), indicators of skeletal muscle damage.

Measurement of ROS

For this assay, the Reactive Oxygen Species (ROS) Assay Kit (E004; Nanjing Jiancheng Bioengineering Institute, Nanjing, China) was used. In this study, C2C12 cells were subjected to treatment and subsequently stained with a concentration of 10μM DCFH-DA for a period of 20–30 minutes. Following that, the cells were observed via a fluorescence microscope (Eclipse TI, Nikon, Tokyo, Japan).

Biochemical Analyses of Malondialdehyde and Superoxide Dismutase Activity

The quantification of Malondialdehyde (MDA) concentration was conducted using a commercially available MDA test kit (Solarbio, China). The measurement of total superoxide dismutase (SOD) activity was assessed via a commercially available SOD kit (Beyotime Institute of Biotechnology, China). The assessment of MDA content and SOD activity was performed using a spectrophotometer, whereby the optical density at wavelengths of 532 nm or 450 nm was compared with standard curves. The determination of total protein concentrations was carried out using a bicinchoninic acid (BCA) assay kit (P0011, Beyotime, Shanghai, China). Moreover, the concentration of MDA was quantified in units of nmol/mg of protein, whereas the activity of SOD was determined as U/mg protein. All experiments were independently repeated three times to ensure reliability.

Assessment of Cell Apoptosis

The evaluation of apoptosis in C2C12 cells was done with the Annexin V-fluorescein isothiocyanate (FITC)/propidium iodide (PI) Apoptosis Detection Kit (Yeasen) and, after that, examined by means of flow cytometry. The C2C12 cells underwent two cycles of cold PBS washing. Subsequently, the cells were once more suspended in a 100 μL solution that contained 5 μL of Annexin V-FITC and 10 μL of PI, in dark. Following a 15-minute incubation period, the cell suspensions underwent analysis utilizing the NovoCyte flow cytometer (ACEA Biosciences). The calculation of the

apoptotic cell percentage involved dividing the count of Annexin V-positive cells by the total cell population and subsequently multiplying it by 100%.

Immunofluorescence Assay

To evaluate the cellular localization of Nrf2, C2C12 cells underwent the following steps: fixation with 4% formaldehyde, single wash with PBS, permeabilization with Triton X-100 (0.1%), and bovine serum albumin (BSA; 1%) prepared in PBS was utilized as a blocking solution. The blocking was done for an hour at ambient temperature. Following that, a primary antibody targeting Nrf2 (dilution of 1:500; Cell signaling, #12721) was added for a duration of 2 h at ambient temperature. After the incubation with the primary antibody, the cells were subjected to treatment with a fluorescent polyclonal secondary antibody at ambient temperature for a duration of 30 minutes. The nuclei were stained with DAPI, and cell imaging was conducted using a fluorescence microscope.

Western Blot Analysis

The process of extracting protein from the skeletal muscle of rats or cells from culture involved the utilization of radioimmunoprecipitation assay lysis buffer (RIPA buffer; Thermo Fisher, MI, USA) according to established protocols.[30] The protein content of each sample was measured with a BCA assay kit (P0011, Beyotime, Shanghai, China). The experiment involved the loading of equivalent amounts of protein onto sodium dodecyl sulfate (SDS) polyacrylamide gels, which were subsequently separated by electrophoresis. After the completion of electrophoresis, the proteins were subsequently deposited onto polyvinylidene difluoride (PVDF) membranes (Sigma-Aldrich, USA). The membranes were initially blocked using a 3% BSA solution at ambient temperature for a duration of 30 minutes. The membranes were then treated with primary antibodies and incubated overnight at 4°C. On the following day, the membranes underwent thrice washes with tris-buffered saline with 0.1% Tween® 20 detergent (TBST) before being subjected to incubation with particular secondary antibodies for 1 h at ambient temperature. The detection of signals was conducted utilizing the Pierce enhanced chemiluminescence (ECL) Kit (Thermo Fisher, USA). The main antibodies utilized in this investigation consisted of the following: anti-AMPKα (Cell signaling, cat# 5832S), anti-PhosphoAMPKα (Cell signaling, cat# 2535), 1:1000; anti-Nrf2 (Abcam, cat# ab31163), 1:1000; anti-HO-1 (Abcam, cat# ab13248), 1:1000; anti-PGC-1α (Abcam, cat# ab13248) 1:1000; anti-IF1 (Cell signaling, cat# 8528), 1:1000; anti-Lamin B1 (Proteintech, cat# 12,987-1-AP), 1:1000; anti-GAPDH (Bioworld, cat# AP0063), 1:5000.

Statistical Analysis

The statistical analysis and graphical depiction were conducted via GraphPad Prism 8.0 (GraphPad Software, USA). The data were reported in the form of mean ± standard error of Mean (SEM). The differences between the treatment groups were assessed by a One-way analysis of variance (ANOVA), which was subsequently followed by the Tukey HSD test. However, if normality test failed, Kruskal–Wallis test with Dunn's test was performed instead. Statistical significance was defined as $p < 0.05$. The sample size was determined according to our preliminary results (histological damage scores). Power analysis was performed using a significance level of $\alpha = 0.05$ with 80% power to detect differences in ANOVA.

Results

BAC Reduces Oxidative Stress and Skeletal Muscle Injury Resulting from I/R in Rats

In order to examine the potential protective impact of BAC against in vivo skeletal muscle injury resulting from I/R of rats, a rat skeletal muscle I/R model was constructed. No animals died during the experiment. The evaluation of muscular tissue damage involved the analysis of morphological alterations observed in H&E stained samples (Figure 1A and B). In the I/R model group, the absence of nuclei, blurred cell boundaries, cytoplasmic fragmentation, and infiltration of neutrophils in the muscular tissue were observed. However, the sham group did not exhibit these changes. As a result, there was a notable increase in histological damage scores in the I/R group compared to the sham group ($P < 0.01$). The administration of BAC to rats subjected to I/R resulted in notable mitigation of muscle damage. This was demonstrated by a decrease in sarcoplasm disintegration, a reduction in the loss of nuclei, and a lowered infiltration of neutrophils, all

of which were seen in comparison to the I/R group. Consequently, BAC reduced histological damage scores in the muscle tissue following I/R injury in a dose-dependent manner ($P < 0.01$). Upon comparison to the sham group, the I/R model group's skeletal muscle wet weight/dry weight (W/D) ratio showed a substantial rise ($P < 0.01$) (Figure 1C). However, treatment with BAC dose-dependently reversed this increase, with the efficacy of BAC at 20 mg/kg being comparable to that of NAC. Furthermore, serum LDH and CK levels, which are indicators of the breakdown of muscle fibers, were substantially higher in rats with I/R in comparison to the sham group ($P < 0.01$). Notably, serum levels of CK and LDH were markedly lowered by BAC therapy in a dose-dependent way ($P < 0.01$). Comparable decreases in serum levels of LDH and CK were also noted in the I/R + NAC group (Figure 1D and E). The evaluation of oxidative stress showed that the I/R group had substantially higher MDA levels and lower SOD activity than the sham group ($P < 0.01$). In contrast to the I/R group, however, BAC therapy successfully decreased levels of MDA and raised the activity of SOD ($P < 0.01$) (Figure 1F and G). Collectively, these findings demonstrate the ability of BAC to mitigate skeletal muscle injury resulting from I/R and ROS accumulation.

BAC Alleviates Apoptosis Induced by I/R in Skeletal Muscle

To evaluate apoptotic levels, a TUNEL staining was conducted to identify cellular apoptosis. The total count of apoptotic cells was substantially increased in rats subjected to I/R in contrast to the sham group ($P < 0.01$) (Figure 2A and B). However, a dose-dependent reduction in apoptotic levels was observed after BAC treatment ($P < 0.01$). WB was used to undertake further examination of the expression levels of cleaved caspase-3, B-cell lymphoma 2 (Bcl-2), and Bcl-2 associated X (Bax). The findings of the study indicated that I/R treatment led to an upregulation of Bax and cleaved caspase-3 expressions in comparison to the sham group ($P < 0.01$). In contrast, BAC administration dramatically and dose-dependently suppressed the elevated expression of Bax and cleaved caspase-3 ($P < 0.01$). Bcl-2 expression was decreased in the I/R group relative to the sham group ($P < 0.01$). Nevertheless, this decrease was efficiently counterbalanced in a dose-dependent way by the BAC treatment ($P < 0.01$) (Figure 2C–F). Collectively, these findings suggest that BAC has a strong inhibitory impact on the apoptosis caused by reperfusion.

BAC Suppresses H/R-Induced C2C12 Cell Injury and Oxidative Stress

The cells of the H/R model group exhibited much lower viability in comparison to the control group (Figure 3A). However, treatment with BAC caused a dose-dependent reversal in this decrease in cell viability ($P < 0.01$). Additionally, the levels of LDH and CK, markers of skeletal muscle injury, were substantially elevated in the H/R group in contrast to the sham group ($P < 0.01$). Notably, BAC therapy dose-dependently decreased the levels of CK and LDH, with the efficacy of BAC at 60 μM being comparable to that of NAC ($P < 0.01$) (Figure 3B and C). Moreover, the presence of ROS was assessed within the cells, and a notable elevation in green fluorescence was observed in the H/R group ($P < 0.01$). However, co-incubation of C2C12 cells with BAC showed a dose-dependent reduction in fluorescence intensity ($P < 0.01$) (Figure 3D and E). The findings regarding ROS levels were further corroborated by the biochemical analysis, which revealed that BAC treatment significantly suppressed MDA activity while augmenting SOD levels upon comparison to the H/R group. ($P < 0.01$, $P < 0.05$) (Figure 3F and G). Collectively, this indicates that BAC ameliorated oxidative stress injury in C2C12 cells.

BAC Reduces H/R-Induced C2C12 Cell Apoptosis

Using flow cytometry assay, the level of apoptosis was checked in C2C12 cells. When compared to the controls, the annexin V-FITC/PI double staining data showed a significant increase in the rate of apoptosis after H/R treatment, which the BAC therapy reversed ($P < 0.01$) (Figure 4A). The findings of the WB assay showed that, in comparison to the control group, the H/R therapy increased the levels of expression of the cleaved caspase-3 and Bax ($P < 0.01$). Nevertheless, the administration of BAC demonstrated a significant ability to inhibit the upregulation of Bax and cleaved caspase-3 expression, with the extent of suppression being dependent on the dosage ($P < 0.01$). Following H/R therapy, Bcl-2 expression was lowered; however, this reduction was dose-dependently offset by BAC administration ($P < 0.01$) (Figure 4B). Taken together, the findings of this study indicate that BAC exhibits a strong inhibitory effect on apoptosis generated by H/R in C2C12 cells.

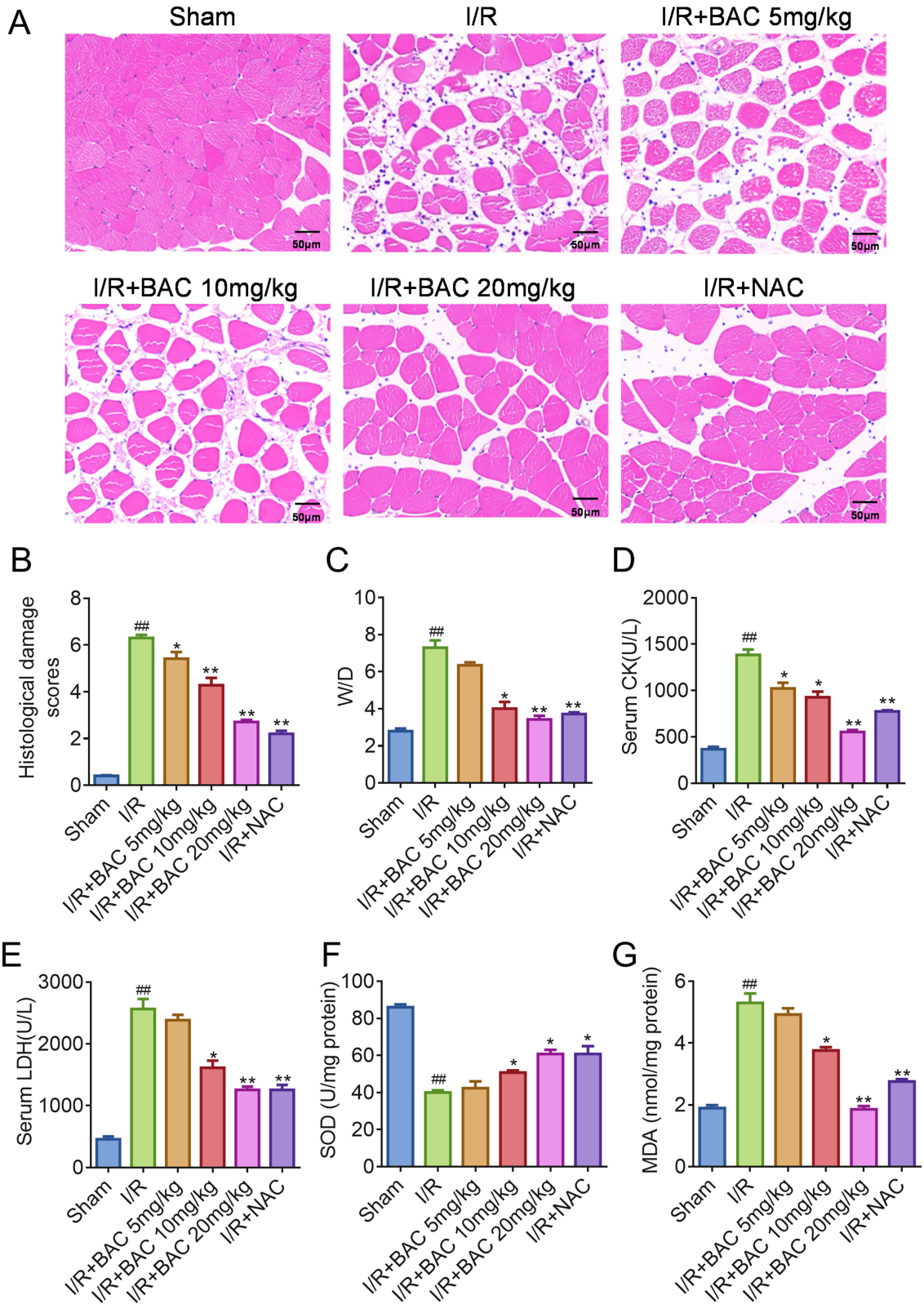

Figure 1 BAC mitigates rat skeletal muscle injury resulting from I/R and oxidative stress damage. (**A**) Representative images of skeletal muscle sections stained with H&E. (**B**) Quantification of histological damage scores. (**C**) W/D ratios for tissue edema of skeletal muscle injury caused by I/R. (**D**) Serum CK level. (**E**) Serum LDH level. (**F**) The SOD activity in the muscle of rats. (**G**) MDA levels in muscle tissue. Here n = 6. The statistical significance levels were denoted as follows: $^{\#\#}$ $p < 0.01$, comparison with the sham group; * $p < 0.05$ and ** $p < 0.01$ comparison with the I/R group.

Abbreviations: I/R, ischemia-reperfusion injury; BAC, Benzoylaconine; NAC, N-acetylcysteine; W/D, weight/dry weight.

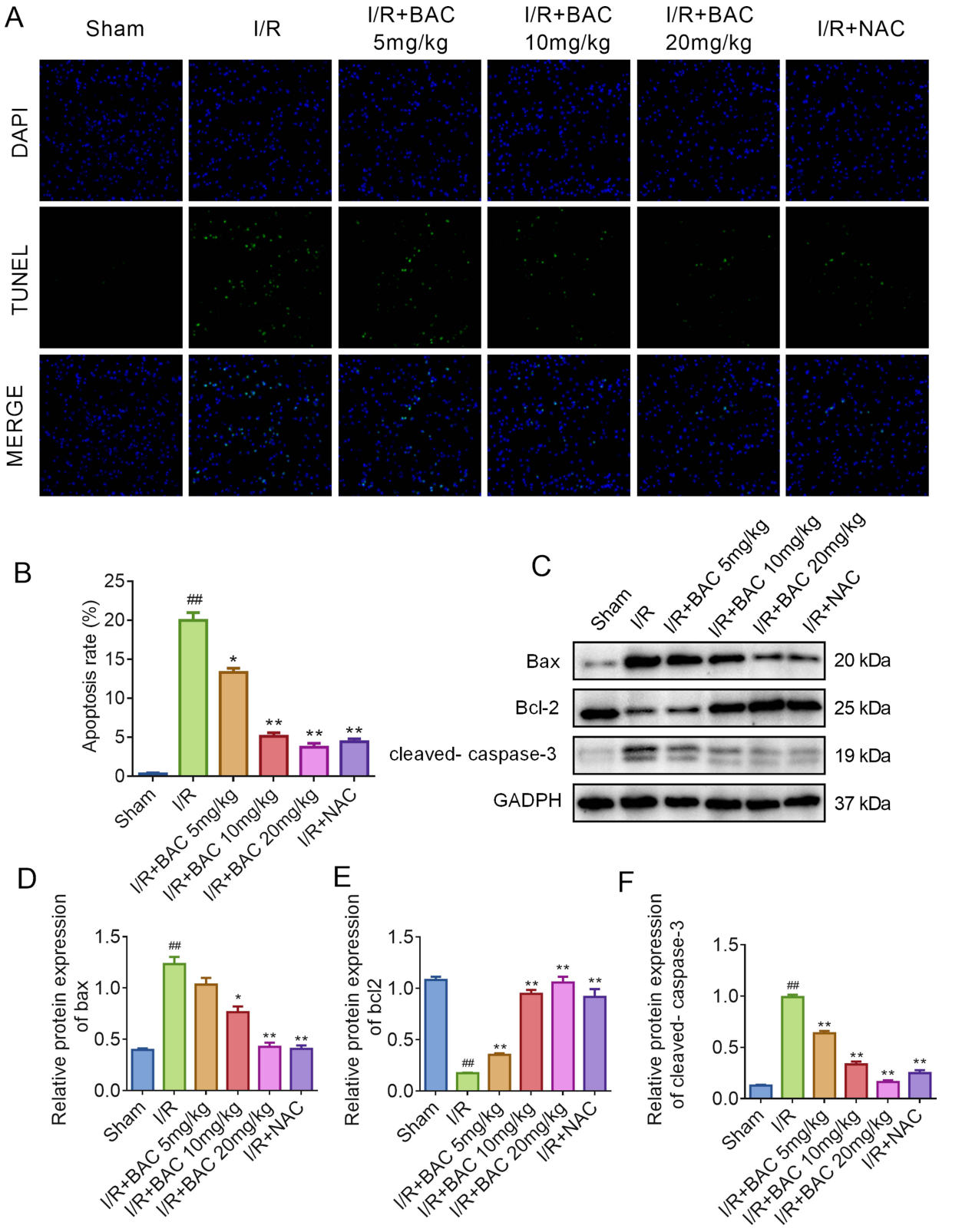

Figure 2 BAC alleviates I/R-induced apoptosis in skeletal muscle. (**A**) Representative images obtained from TUNEL assay of skeletal muscle sections and (**B**) corresponding quantitative analysis. TUNEL-positive cells were visualized green, while DAPI staining appeared as blue under fluorescence microscopy. (**C**) WB and quantitative analysis of Bax (**D**), Bcl-2 (**E**), and cleaved caspase 3 (**F**) levels in muscle tissue. The statistical significance levels were denoted as follows: $^{\#\#}$ $p < 0.01$, comparison with the sham group; * $p < 0.05$ and ** $p < 0.01$ comparison with the I/R group.

Abbreviations: I/R, ischemia-reperfusion injury; BAC, Benzoylaconine; NAC, N-acetylcysteine.

https://doi.org/10.2147/DDDT.S456699 DovePress

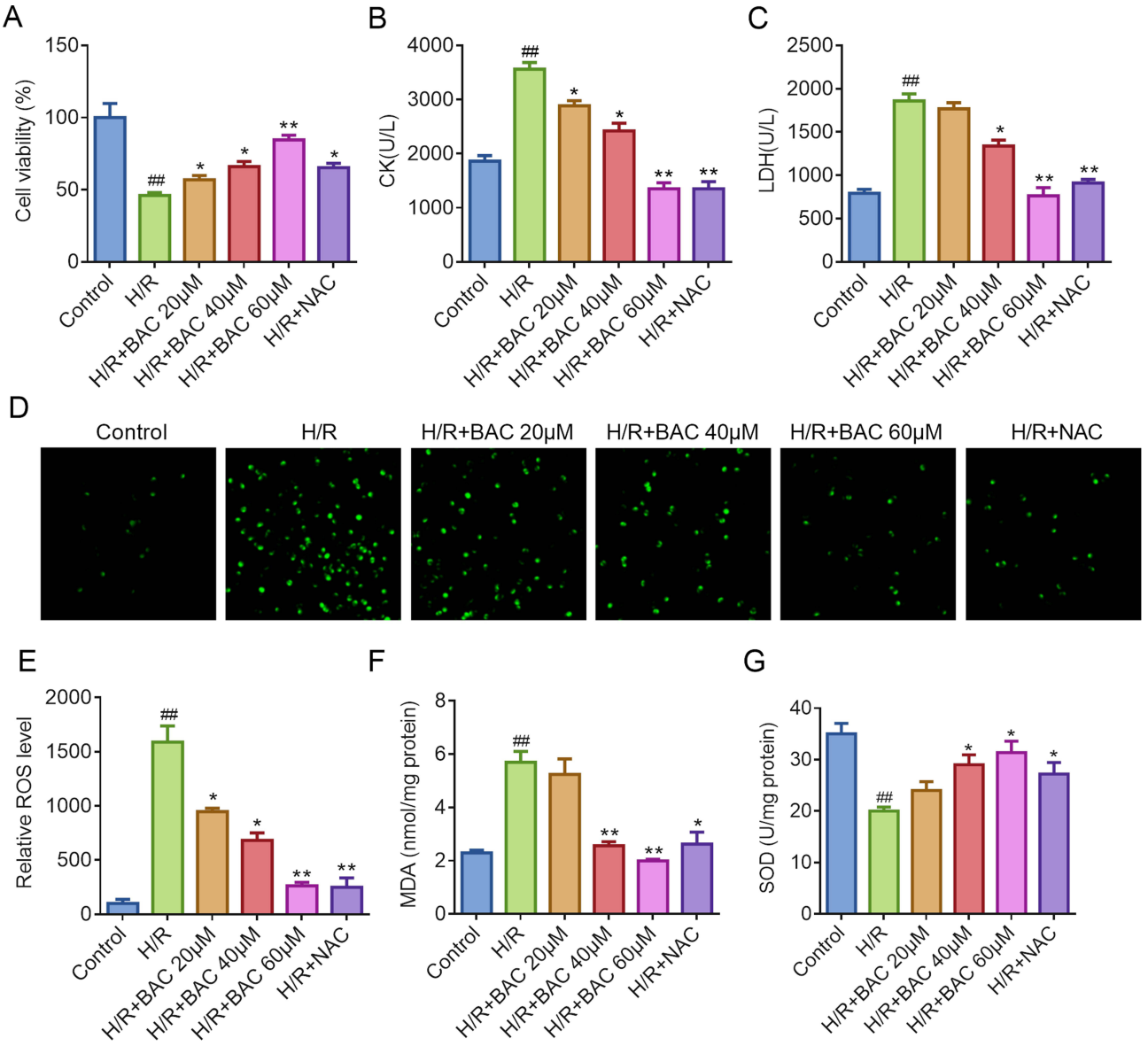

Figure 3 BAC suppresses H/R-induced C2C12 cell injury and oxidative stress. (**A**) The cell viability was assessed. (**B**) CK release for assessing the extent of cellular injury (**C**) LDH release to assess the level of cell injury. (**D**) ROS generation was measured using the DCFH-DA assay. (**E**) Quantitative analysis of ROS level. (**F**) MDA activity detected by assay kits. (**G**) SOD levels detected by assay kits. Here n = 3. The statistical significance levels were denoted as follows: $^{\#\#}$ $p < 0.01$, comparison with the sham group; * $p < 0.05$ and ** $p < 0.01$ comparison with the H/R group.

Abbreviations: H/R, hypoxia/reoxygenation; BAC, Benzoylaconine; NAC, N-acetylcysteine.

BAC Treatment Activated AMPK/Nrf2 and AMPK/ PGC-1α Axis in H/R-Treated C2C12 Cells

Nrf2, a crucial regulator of redox homeostasis, serves as the cellular target for numerous antioxidant natural compounds.[31] To investigate whether BAC activates the Nrf2 signaling pathway, we examined C2C12 cell samples treated with BAC using specific antibodies for Nrf2 and HO-1. Nrf2 levels in the nucleus increased as a result of BAC treatment ($P < 0.01$) (Figures 5A–D and 5E). Concurrently, an increase in levels of HO-1 was observed in response to BAC treatment ($P < 0.01$) (Figure 5A–C). Notably, these changes in the expression of HO-1 and Nrf2 exhibited a dose-dependent pattern following BAC treatment. To further confirm the activation of nuclear translocation of Nrf2 by BAC, an immunofluorescence assay was performed to visualize the distribution of Nrf2 within the nucleus (Figure 5F). Enhanced co-staining of Nrf2 and DAPI was evident in cellular samples that underwent pre-treatment with BAC in

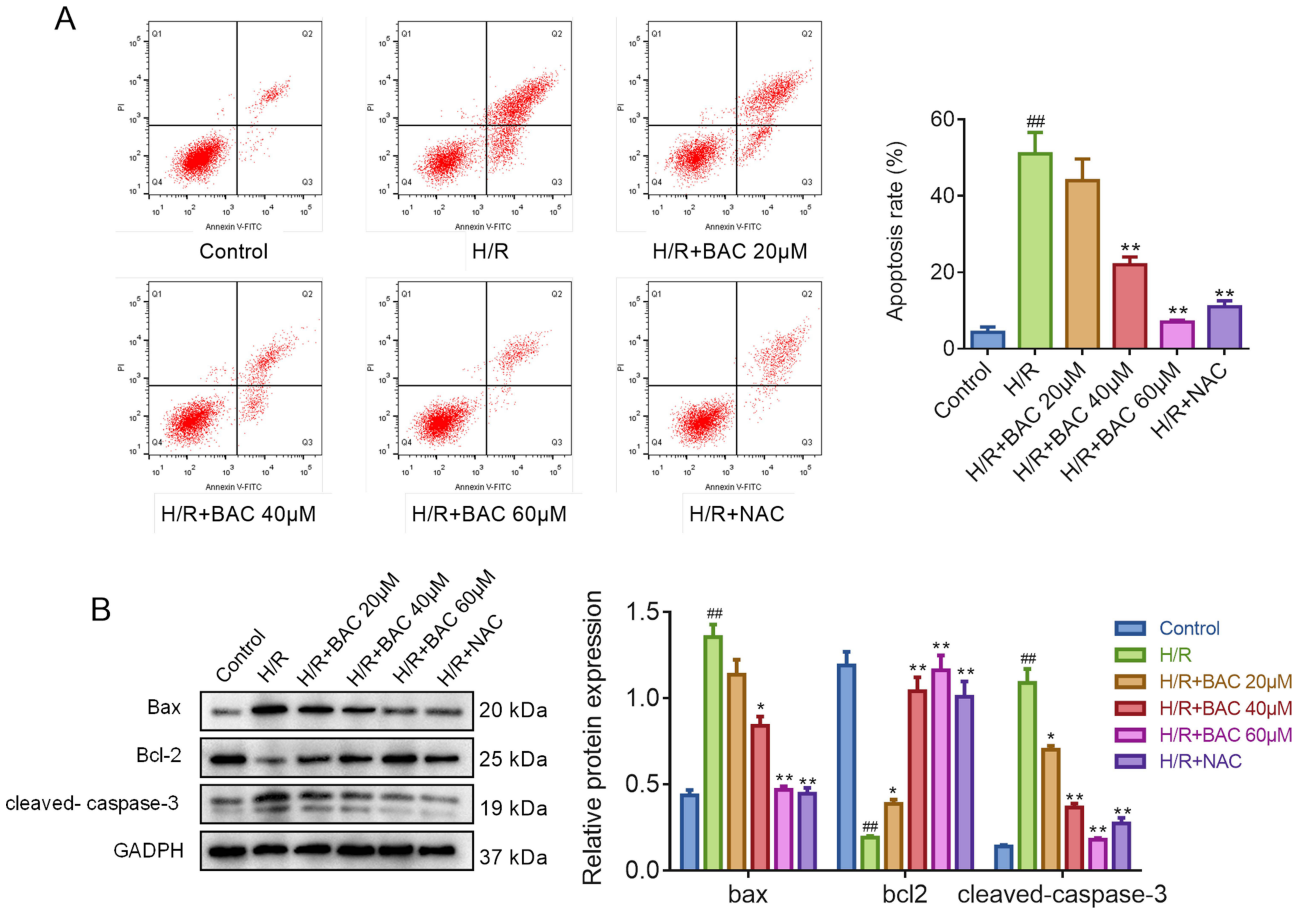

Figure 4 BAC decreases the C2C12 cells' H/R-induced apoptosis. (**A**) Assessment of C2C12 cell apoptosis via flow cytometry and Annexin V/PI (**B**) H/R-induced C2C12 cells were subjected to WB and quantitative measurement of Bcl-2, cleaved caspase 3, and Bax levels. Here n = 3. The statistical significance levels were denoted as follows: ## $p < 0.01$, comparison with the sham group; * $p < 0.05$ and ** $p < 0.01$ comparison with the H/R group.
Abbreviations: H/R, hypoxia/reoxygenation; BAC, Benzoylaconine; NAC, N-acetylcysteine.

comparison to the non-BAC-treated cells. Interestingly, it was also shown that phosphorylation of AMPK was induced in the presence of BAC in a dose-dependent way ($P < 0.01$) (Figure 5A and B). In summary, the outcomes demonstrate that BAC activates the AMPK/Nrf2 axis in H/R-treated C2C12 cells.

PGC-1α is another downstream molecule of AMPK and is known to participate in mitochondrial biogenesis. Therefore, we further evaluated the expression level of PGC-1α. As a result, BAC treatment dose-dependently increased PGC-1α expression compared to the H/R group ($P < 0.01$) (Figure 5G), indicating that BAC activates the AMPK/PGC-1α axis in H/R-treated C2C12 cells.

Inhibition of AMPK Reversed the BAC-Mediated Translocation of Nuclear Nrf2 and Myocyte-Protective Effects of BAC

AMPK, a heterotrimeric protein complex, is considerably important in regulating cellular energy metabolism.[32] Recent evidence has unveiled the interplay between AMPK and Nrf2 pathways.[33] Following its activation, AMPK phosphorylates Nrf2 at several serine sites, hence promoting its nuclear translocation.[31] To investigate the possible role of AMPK in the activation of the Nrf2/HO-1 pathway by BAC therapy, it was necessary to conduct a comprehensive analysis. Therefore, the cells were subjected to treatment with Compound C, a particular antagonist targeting AMPK, followed by BAC treatment. The results of immunofluorescence and WB assay demonstrated that inhibiting AMPK with Compound C significantly suppressed the nuclear accumulation of Nrf2 and the upregulation of HO-1 expression induced by BAC ($P < 0.01$) (Figure 6A–C). These outcomes indicate that BAC stimulates the signaling pathway of Nrf2/HO-1 in a manner that is dependent on AMPK.

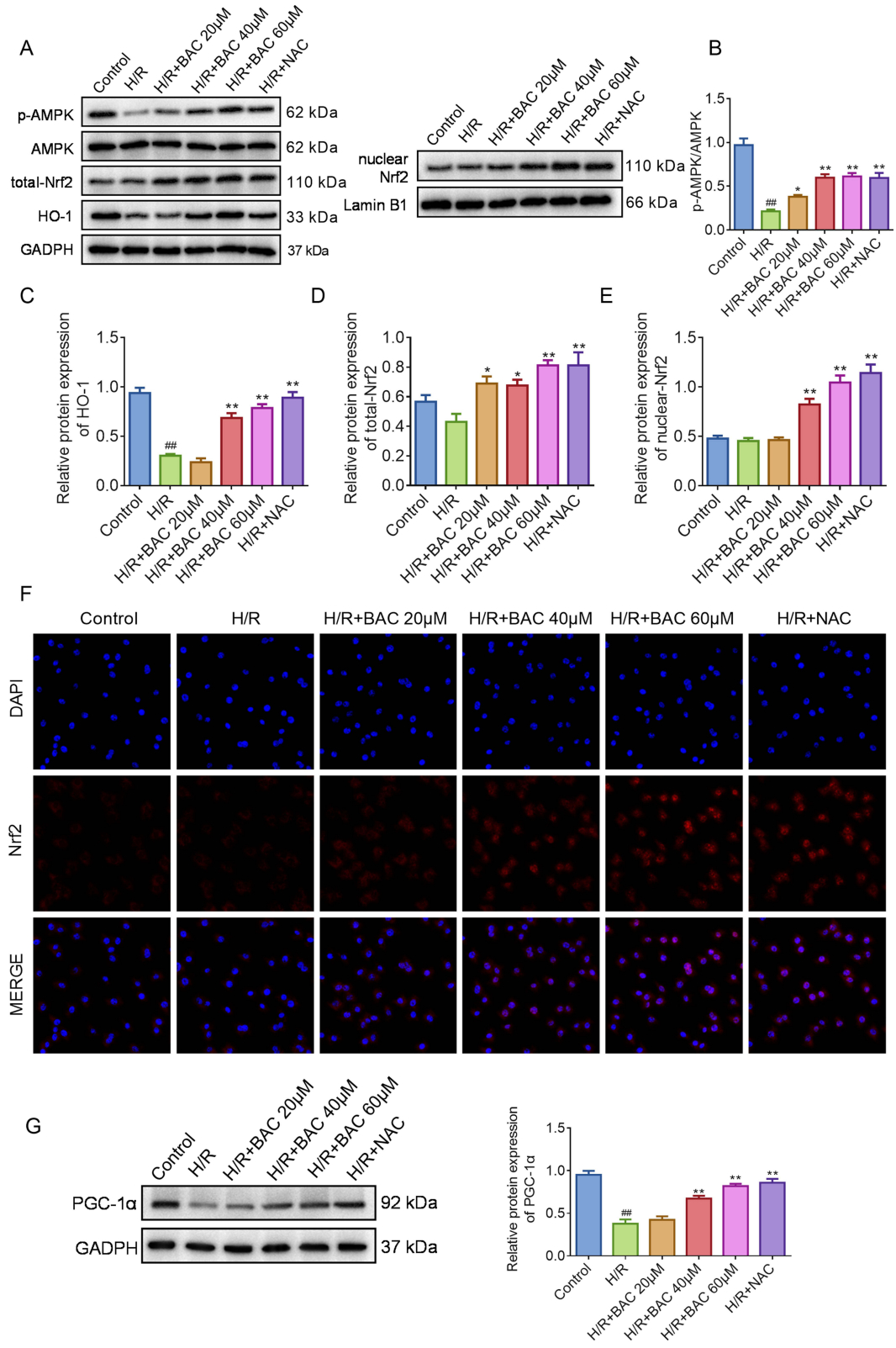

Figure 5 BAC treatment activated the AMPK/Nrf2 axis in H/R-treated C2C12 cells. (**A**) Representative WB bands of phosphorylated AMPK, AMPK, Nrf2, and HO-1. (**B**) p-AMPK/AMPK quantitative analysis (**C**) HO-1 quantitative analysis. (**D**) Total Nrf2 quantitative analysis. (**E**) Nuclear Nrf2 quantitative analysis. (**F**) Subcellular distribution of Nrf2 was assessed using immunofluorescence staining. Nrf2 was visualized as red fluorescence, while the cell nuclei were stained blue. (**G**) Quantitative analysis and WB of PGC-1α level. Here n = 3. The statistical significance levels were denoted as follows: $^{\#\#}$ $p < 0.01$, comparison with the sham group; * $p < 0.05$ and ** $p < 0.01$ comparison with the H/R group.

Abbreviations: H/R, hypoxia/reoxygenation; BAC, Benzoylaconine; NAC, N-acetylcysteine.

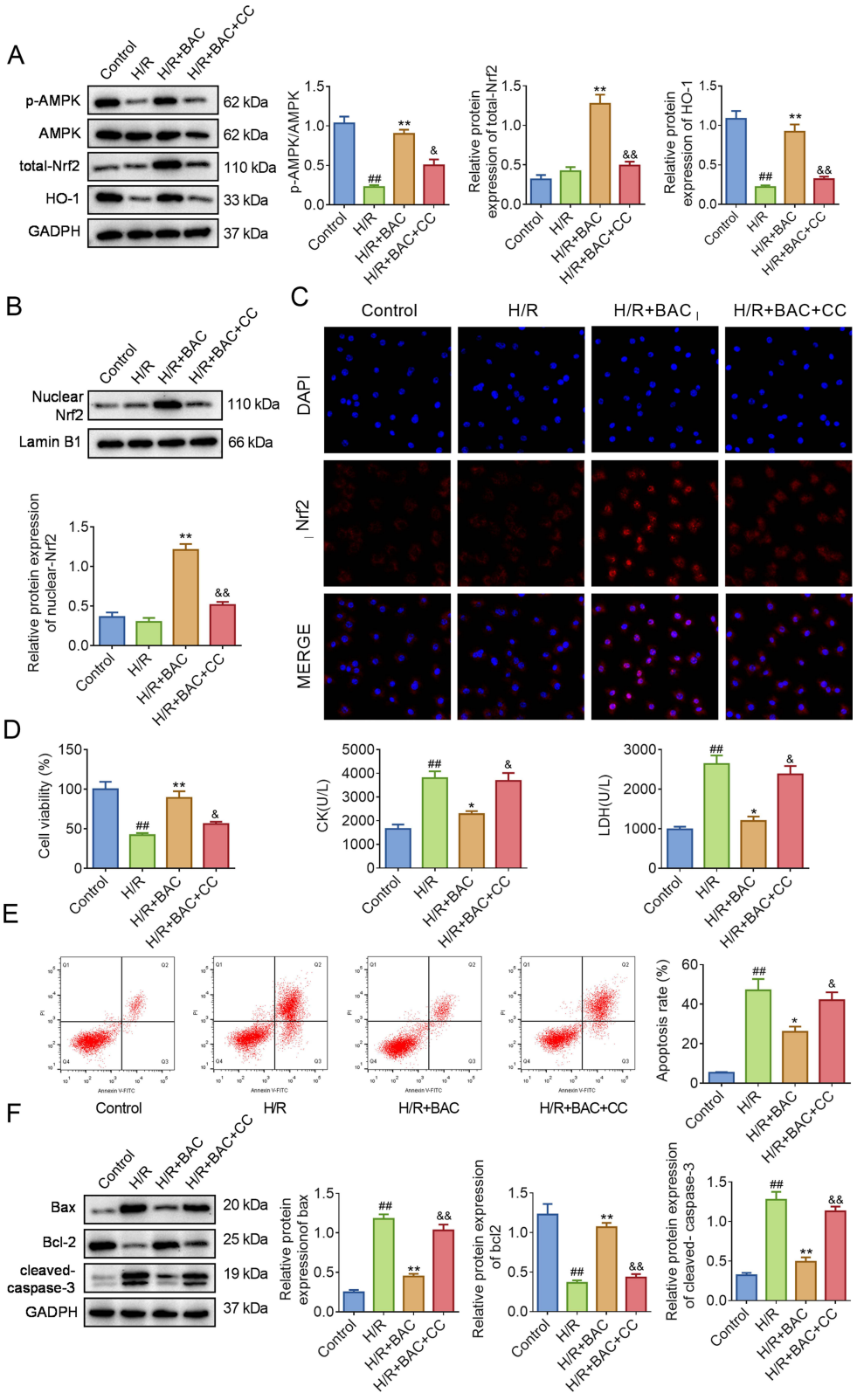

Figure 6 Inhibition of AMPK abolished the BAC-mediated translocation of nuclear Nrf2 and myocyte-protective impact of BAC. (**A**) In H/R-induced C2C12 cells, quantitative measurement and WB of total Nrf2, HO-1, and p-AMPK/AMPK levels. (**B**) Quantitative analysis and WB of nuclear Nrf2 levels. (**C**) Subcellular distribution of Nrf2 was assessed using immunofluorescence staining. (**D**) Cell viability as well as CK and LDH release for evaluating the degree of cell damage. (**E**) Assessing cell apoptosis using flow cytometry and Annexin V/PI. (**F**) H/R-induced C2C12 cells were subjected to WB and quantitative measurement of Bax, Bcl-2, and cleaved caspase 3 levels. Here n = 3. The statistical significance levels were denoted as follows: $^{\#\#}$ $p < 0.01$, comparison with the sham group; * $p < 0.05$ and ** $p < 0.01$ comparison with the H/R group; $^{\&}$ $p < 0.05$ and $^{\&\&}$ $p < 0.01$ comparison with the H/R + BAC group.

Abbreviations: H/R, hypoxia/reoxygenation; BAC, Benzoylaconine; CC, Compound C.

https://doi.org/10.2147/DDDT.S456699 DovePress

Based on the significant involvement of the Nrf2/HO-1 pathway in counteracting oxidative damage, it was speculated that the protective effects of BAC on myocytes can be attributed to the activation of AMPK/Nrf2. To evaluate the myocyte-protective effect of BAC, pre-treatment was conducted with Compound C. As shown in Figure 6D, pre-treatment with Compound C abolished the BAC-induced decrease in CK and LDH levels and increased cell viability ($P < 0.01$, $P < 0.05$). Consistently, Compound C also antagonized the anti-apoptotic actions of BAC, as evidenced by the results of annexin V-FITC/PI double staining and the Bcl-2, Bax, and cleaved caspase3 expression levels ($P < 0.05$, $P < 0.01$) (Figure 6E and F). The results of this study validate the notion that AMPK/Nrf2 activation is responsible for the antioxidative ability and myocyte-protective effects of BAC.

Silencing of IF1 Abolished BAC-Induced Activation of AMPK/Nrf2 Axis

To have a thorough comprehension of the regulatory process by which BAC affects the AMPK/Nrf2 axis, we investigated the potential involvement of IF1, known to stimulate AMPK activation.[25,26] The IF1 protein was substantially reduced as a result of using H/R treatment, whereas BAC treatment dose-dependently increased IF1 expression in contrast to the H/R group ($P < 0.01$) (Figure 7A). To conduct an extensive investigation regarding the regulatory function of IF1 in the AMPK/Nrf2 axis, we performed knockdown experiments. WB assay verified the successful knockdown of IF1 expression in C2C12 cells (Figure 7B). Subsequently, the impact of IF1 knockdown on the BAC-induced activation of the AMPK/Nrf2 axis was assessed. As shown in Figure 7C and D, the WB analysis indicated that the downregulation of IF1 successfully eliminated the elevation in AMPK phosphorylation in the presence of BAC ($P < 0.01$). Correspondingly, the BAC-induced nuclear translocation of Nrf2 and the subsequent upregulation in the expression of HO-1 were also blocked by IF1 knockdown ($P < 0.01$) (Figure 7C, 7E–G). The immunofluorescence assay provided evidence that the nuclear translocation of Nrf2 was hindered in the H/R + BAC + SiIF1 group, as opposed to the H/R + BAC + SiF1-NC group. This finding is consistent with the data obtained from the WB analysis (Figure 7H). These findings collectively suggest the involvement of IF1 in BAC-mediated stimulation of the AMPK/Nrf2 axis.

Discussion

The present investigation yielded noteworthy findings. Initially, an experimental rat model was employed to demonstrate the preventive effect of BAC treatment on skeletal muscle injury caused by I/R. Furthermore, the administration of BAC resulted in increased viability of cells in H/R-induced C2C12 cells, mitigated oxidative stress injury, and attenuated apoptosis caused by H/R. Furthermore, the protective effect of BAC on myocytes was shown to be impeded in the presence of AMPK/Nrf2 pathway inhibition. Lastly, BAC-induced upregulation of the AMPK/Nrf2 pathway in C2C12 cells relied on the presence of IF1. Overall, the current study establishes BAC as a possible therapeutic agent for safeguarding myocytes from skeletal muscle injury resulting from I/R and reveals a novel mechanism whereby BAC's elevation of IF1/AMPK-dependent antioxidative stress function contributes to its myocyte-protective role.

The precise molecular processes behind I/R injury remain elusive; nonetheless, it has been postulated that apoptosis, oxidative stress, and inflammation have a substantial part in the development of I/R injury.[5,34] Excessive mitochondrial fission-induced apoptosis has been recognized as a pivotal factor in I/R damage.[35] Importantly, the recanalization of ischemic skeletal muscle has been linked to various injurious reactions, including apoptosis.[19] Studies have underscored the exacerbating effect of heightened oxidative stress on myocyte apoptosis.[36] BAC, which originates from *Aconitum carmichaelii* Debeaux, a frequently prescribed Chinese medicinal plant, has demonstrated anti-inflammatory and antioxidant characteristics in prior studies.[8,9] While there has been recent exploration into the protective function of BAC in cardiac I/R injury,[37] its possible protective impacts on skeletal muscle injury resulting from I/R are yet unknown. In the current study, the protective effects of BAC against skeletal muscle I/R injury have been demonstrated through reduced histopathological lesions, tissue edema (W/D), CK, and LDH levels in vivo, as well as enhanced cell viability. According to the study's findings, BAC may be utilized as a preventive agent for protecting against I/R injury. Additionally, BAC exhibited antioxidant and antiapoptotic effects both in vivo and in vitro, highlighting its myocyte-protective function through these mechanisms.

The transcription factor Nrf2 plays a pivotal function in protecting against harm caused by oxidative stress.[38] Upon exposure to oxidative stress, the transcription factor Nrf2 dissociates from Keap1, a protein associated with Kelch-like ECH, and relocates to the nucleus. In the nucleus, Nrf2 binds to specific regions known as antioxidant response elements

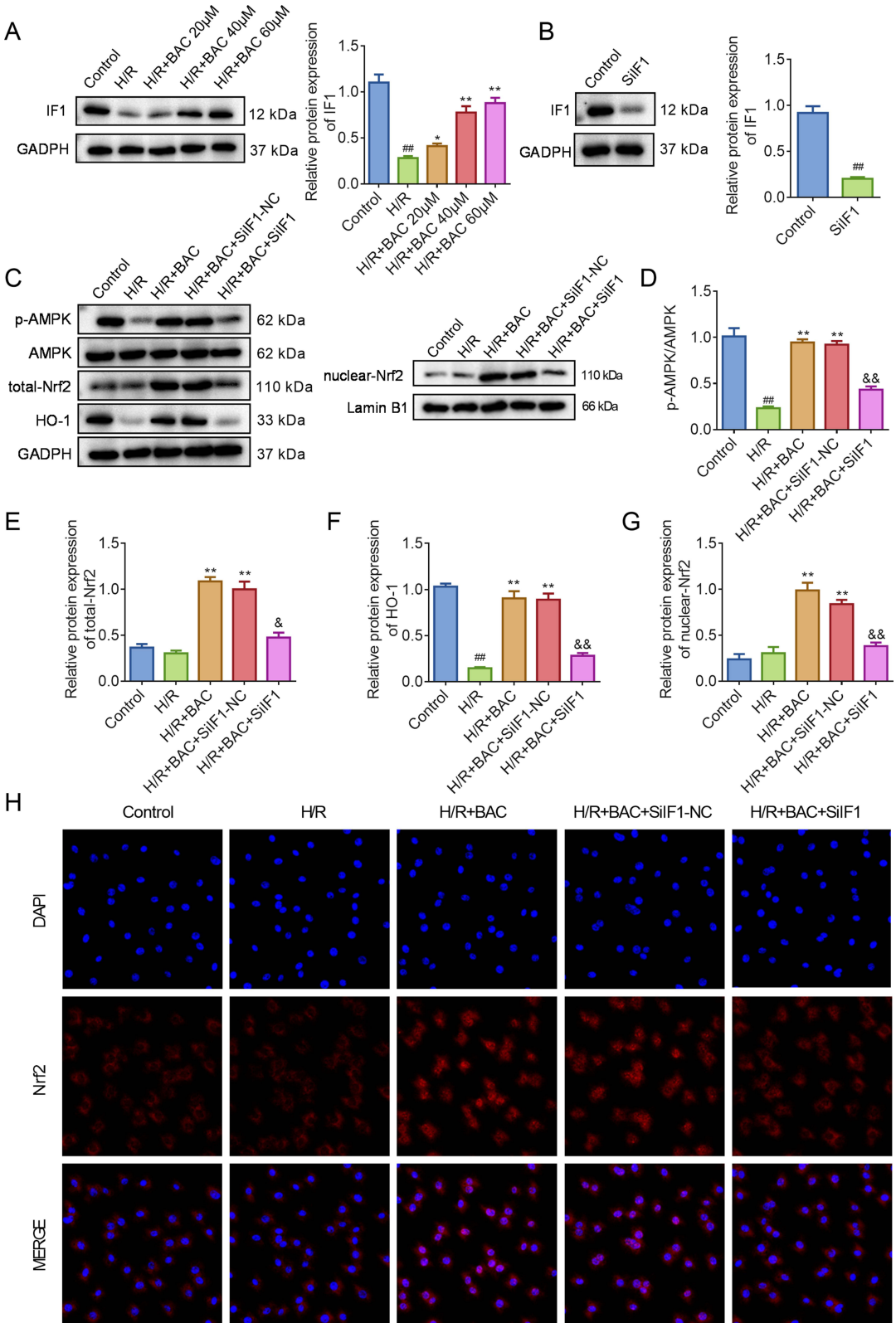

Figure 7 BAC induces the AMPK/Nrf2 axis through the up-regulation of IF1 expression. (**A**) WB and quantitative analysis of IF1 expression following BAC treatment in H/R-treated C2C12 cells. (**B**) WB and quantitative analysis of IF1 expression following IF1 knockdown by siRNA. (**C**) Representative WB bands of phosphorylated AMPK, AMPK, Nrf2, and HO-1. (**D**) Quantitative analysis of p-AMPK/AMPK. (**E**) Total Nrf2 quantitative analysis. (**F**) HO-1 quantitative analysis. (**G**) Nuclear Nrf2 quantitative analysis. (**H**) Subcellular distribution of Nrf2 was assessed using immunofluorescence staining. Here n = 3. The statistical significance levels were denoted as follows: $^{\#\#}$ $p < 0.01$, comparison with the sham group; * $p < 0.05$ and ** $p < 0.01$ comparison with the H/R group; $^{\&}$ $p < 0.05$ and $^{\&\&}$ $p < 0.01$ comparison to the H/R + BAC + SiF1-NC group.
Abbreviations: H/R, hypoxia/reoxygenation; BAC, Benzoylaconine.

https://doi.org/10.2147/DDDT.S456699 DovePress

(ARE) and triggers the activation of downstream antioxidant defense enzymes, including HO-1.[39,40] Numerous studies have demonstrated that disruption of Nrf2 results in an increased number of apoptotic cells in skeletal muscle during I/R injury and aging skeletal myocytes.[29] BAC was shown to have myocyte-protective effects in the present research via increasing Nrf2's nuclear translocation and raising HO-1 levels. These results point to a possible connection between the Nrf2-mediated antioxidant response and the protective function of BAC in skeletal muscle injury caused by I/R.

AMPK, a serine/threonine protein kinase, plays a crucial role in the regulation of cellular stress and energy balance. It has been demonstrated to be a significant contributor to oxidative damage and inflammation.[41] Additionally, upon activation, AMPK phosphorylates Nrf2, resulting in its detachment from Keap1 and subsequent relocation to the cellular nucleus.[31] The pathway of AMPK is a widely distributed signaling system that has been involved in the activation of Nrf2 and the antioxidant capabilities of natural substances.[42,43] This study aimed to examine the impact of BAC therapy on the phosphorylation of AMPK, revealing a correlation that is contingent upon the administered dosage. Furthermore, we inhibited AMPK using Compound C and observed that this reversed the beneficial effects of BAC on myocyte protection. Specifically, inhibition of AMPK increased apoptosis while also reducing BAC-mediated Nrf2 nuclear translocation and expression of HO-1. The results of the current study indicate that the activation of the Nrf2/HO-1 pathway by BAC is dependent upon the activation of AMPK.

How does BAC facilitate AMPK activation? The activity of AMPK is regulated by the ratios of AMP/ATP or ADP/ATP.[43] Under acidic conditions like myocardial ischemia, IF1, a nuclear-encoded protein that interacts with ATP synthase, acts as an inhibitor of ATP synthase hydrolysis activity.[44,45] IF1 has been shown in the alteration of energy metabolism since it promotes glycolysis by restricting ATP generation through F1F0-ATP synthase in both cell culture and tissue-specific mice models.[46,47] Additionally, prior research has demonstrated that reducing IF1 levels through siRNA-mediated knockdown increases ATP levels and subsequently enhances insulin secretion in pancreatic β-cell models.[48] IF1 has also been shown to activate AMPK signaling in both I/R hearts and H/R cardiomyocytes.[26] The findings presented in this research revealed a positive correlation between the dosage of BAC therapy and the increased expression of IF1. In addition, the use of siRNA to reduce the expression of IF1 resulted in the elimination of AMPK activation triggered by BAC, as well as the translocation of Nrf2 to the nucleus and the consequent increase in the production of HO-1. The aforementioned collective data provide evidence that BAC promotes the activation of the AMPK/Nrf2 axis by increasing the expression of IF1.

Our study had several limitations. Firstly, in order to control for variations in the endocrine system and ensure consistency in the experimental results, we only used male mice. However, future research should consider including female animals to account for gender differences. Second, we did not evaluate the blood flow in the hind limb, which could have offered valuable insights into the ischemic condition. Nevertheless, many studies have validated the effectiveness of the ischemia-reperfusion model induced by microvascular clamps and elastic tourniquets in hind limbs. Lastly, a prior study demonstrated that BAC modulated mitochondrial function in cardiomyocyte injury induced by oxygen-glucose deprivation and reperfusion by activating the AMPK/PGC-1α axis.[37] Our study revealed that BAC significantly reduced PGC-1α expression in a dose-dependent manner in H/R-treated myocytes. Therefore, BAC may exert effects on skeletal muscle I/R injury by modulating mitochondrial function. Consequently, further research is necessary to gain a comprehensive understanding of the pleiotropic effects of BAC.

Conclusion

Collectively, the present work offers persuasive data supporting the advantageous impact of BAC in safeguarding skeletal muscle against I/R injury. The study's findings suggest that BAC may be used as a supplemental and alternative therapy that is effective in treating skeletal muscle injury caused by I/R. In addition, a possible mechanism that explains the protective potential of BAC on myocytes during skeletal muscle I/R injury has been explained. This mechanism involves the IF1/AMPK/Nrf2 axis and its ability to mitigate oxidative stress.

Data Sharing Statement

The data underlying this article will be shared upon reasonable request to the corresponding author.

Funding

This work was financially supported by the Program of Outstanding Academic Leader of Shanghai Science and Technology Commission (22XD1422200).

Disclosure

The authors report no conflicts of interest in this work.

References

1. Morikawa T, Shimasaki M, Ichiseki T, Ueda S, Ueda Y, Takahashi K. The possibility of IPC to prevent ischemic-reperfusion injury in skeletal muscle in a rat. *J Clin Med*. 2023;12(4):1501. doi:10.3390/jcm12041501
2. Erol K, Sozmen EY, Küçük Ü, Kucuk L. Effect of pheniramine maleate on rat skeletal muscle ischemia-reperfusion injury. *Ulus Travma Acil Cerrahi Derg*. 2022;28(12):1667–1673. doi:10.14744/tjtes.2021.00312
3. Murray IR, Gonzalez ZN, Baily J, et al. αv integrins on mesenchymal cells regulate skeletal and cardiac muscle fibrosis. *Nat Commun*. 2017;8(1):1118. doi:10.1038/s41467-017-01097-z
4. Li Y, Jiang J, Tong L, et al. Bilobalide protects against ischemia/reperfusion-induced oxidative stress and inflammatory responses via the MAPK/NF-κB pathways in rats. *BMC Musculoskeletal Dis*. 2020;21(1):449. doi:10.1186/s12891-020-03479-9
5. Li B, Liu L. Fibroblast growth factor 21, a stress regulator, inhibits Drp1 activation to alleviate skeletal muscle ischemia/reperfusion injury. *Lab Invest*. 2022;102(9):979–988. doi:10.1038/s41374-022-00787-7
6. Zhang QQ, Chen FH, Wang F, Di XM, Li W, Zhang H. A novel modulator of the renin-angiotensin system, benzoylaconitine, attenuates hypertension by targeting ACE/ACE2 in enhancing vasodilation and alleviating vascular inflammation. *Front Pharm*. 2022;13:841435. doi:10.3389/fphar.2022.841435
7. Xu YW, Xu ZD, An R, Zhang H, Wang XH. Revealing the synergistic mechanism of Shenfu Decoction for anti-heart failure through network pharmacology strategy. *Chin J Nat Med*. 2020;18(7):536–549. doi:10.1016/s1875-5364(20)30064-9
8. Zhou C, Gao J, Ji H, et al. Benzoylaconine modulates LPS-induced responses through inhibition of toLl-like receptor-Mediated NF-κB and MAPK Signaling in RAW264.7 Cells. *Inflammation*. 2021;44(5):2018–2032. doi:10.1007/s10753-021-01478-z
9. Deng XH, Liu JJ, Sun XJ, Dong JC, Huang JH. Benzoylaconine induces mitochondrial biogenesis in mice via activating AMPK signaling cascade. *Acta Pharmacol Sin*. 2019;40(5):658–665. doi:10.1038/s41401-018-0174-8
10. Zhang H, Wu Q, Li W, et al. Absorption and metabolism of three monoester-diterpenoid alkaloids in Aconitum carmichaeli after oral administration to rats by HPLC-MS. *J Ethnopharmacol*. 2014;154(3):645–652. doi:10.1016/j.jep.2014.04.039
11. Zhang H, Liu M, Zhang W, et al. Comparative pharmacokinetics of three monoester-diterpenoid alkaloids after oral administration of Acontium carmichaeli extract and its compatibility with other herbal medicines in Sini Decoction to rats. *Biomed Chromatogr*. 2015;29(7):1076–1083. doi:10.1002/bmc.3394
12. Zhang W, Zhang H, Sun S, et al. Comparative pharmacokinetics of hypaconitine after oral administration of pure hypaconitine, Aconitum carmichaelii extract and Sini Decoction to rats. *Molecules*. 2015;20(1):1560–1570. doi:10.3390/molecules20011560
13. Zhang H, Sun S, Zhang W, et al. Biological activities and pharmacokinetics of aconitine, benzoylaconine, and aconine after oral administration in rats. *Drug Test Anal*. 2016;8(8):839–846. doi:10.1002/dta.1858
14. Wada K, Nihira M, Hayakawa H, Tomita Y, Hayashida M, Ohno Y. Effects of long-term administrations of aconitine on electrocardiogram and tissue concentrations of aconitine and its metabolites in mice. *Forensic Sci Int*. 2005;148(1):21–29. doi:10.1016/j.forsciint.2004.04.016
15. Madhavi YV, Gaikwad N, Yerra VG, Kalvala AK, Nanduri S, Kumar A. Targeting AMPK in diabetes and diabetic complications: Energy homeostasis, autophagy and mitochondrial health. *Curr Med Chem*. 2019;26(27):5207–5229. doi:10.2174/0929867325666180406120051
16. Jia J, Bissa B, Brecht L, et al. AMPK, a regulator of metabolism and autophagy, is activated by lysosomal damage via a novel galectin-directed ubiquitin signal transduction system. *Mol Cell*. 2020;77(5):951–969.e9. doi:10.1016/j.molcel.2019.12.028
17. Zhao P, Sun X, Chaggan C, et al. An AMPK-caspase-6 axis controls liver damage in nonalcoholic steatohepatitis. *Science*. 2020;367:(6478):652–660. doi:10.1126/science.aay0542
18. Li C, Chi J, Dai H, et al. Salidroside attenuates cerebral ischemia/reperfusion injury by regulating TSC2-induced autophagy. *Exp Brain Res*. 2023;241(1):113–125. doi:10.1007/s00221-022-06493-6
19. Yu H, Hong X, Liu L, et al. Cordycepin Decreases Ischemia/Reperfusion Injury in Diabetic Hearts via Upregulating AMPK/Mfn2-dependent mitochondrial fusion. *Front Pharmacol*. 2021;12:754005. doi:10.3389/fphar.2021.754005
20. Zhao B, G-P L, Peng -J-J, et al. Schizandrin B attenuates hypoxia/reoxygenation injury in H9c2 cells by activating the AMPK/Nrf2 signaling pathway. *Exp Ther Med*. 2021;21(3):220. doi:10.3892/etm.2021.9651
21. Li J, Zheng X, Ma X, et al. Melatonin protects against chromium(VI)-induced cardiac injury via activating the AMPK/Nrf2 pathway. *J Inorg Biochem*. 2019;197:110698. doi:10.1016/j.jinorgbio.2019.110698
22. Tang C, Hong J, Hu C, et al. Palmatine Protects against Cerebral Ischemia/Reperfusion Injury by Activation of the AMPK/Nrf2 Pathway. *Oxid Med Cell Longev*. 2021;2021:1–12. doi:10.1155/2021/6660193
23. Jiang W, Song J, Zhang S, Ye Y, Wang J, Zhang Y. CTRP13 Protects H9c2 Cells Against Hypoxia/Reoxygenation (H/R)-Induced Injury Via Regulating the AMPK/Nrf2/ARE Signaling Pathway. *Cell Transplant*. 2021;30:9636897211033275. doi:10.1177/09636897211033275
24. Lee HJ, Moon J, Chung I, et al. ATP synthase inhibitory factor 1 (IF1), a novel myokine, regulates glucose metabolism by AMPK and Akt dual pathways. *FASEB J*. 2019;33(12):14825–14840. doi:10.1096/fj.201901440RR
25. Faccenda D, Gorini G, Jones A, et al. The ATPase Inhibitory Factor 1 (IF1) regulates the expression of the mitochondrial Ca2+ uniporter (MCU) via the AMPK/CREB pathway. *Biochim Biophys Acta*. 2021;1868(1):118860. doi:10.1016/j.bbamcr.2020.118860
26. J-W W, Hu H, J-s H, L-K M. ATPase inhibitory factor 1 protects the heart from acute myocardial ischemia/reperfusion injury through activating AMPK signaling pathway. *Int J Biol Sci*. 2022;18(2):731–741. doi:10.7150/ijbs.64956
27. Kahancová A, Sklenář F, Ježek P, Dlasková A. Overexpression of native IF1 downregulates glucose-stimulated insulin secretion by pancreatic INS-1E cells. *Sci Rep*. 2020;10(1):1551. doi:10.1038/s41598-020-58411-x

28. He J, He L, Lu F, Geng B, Xia Y. Low-molecular-weight heparin calcium attenuates the tourniquet-induced ischemia-reperfusion injury in rats. *Injury*. 2021;52(8):2068–2074. doi:10.1016/j.injury.2021.03.006
29. Zhang M, Zhang M, Wang L, et al. Activation of cannabinoid type 2 receptor protects skeletal muscle from ischemia-reperfusion injury partly via Nrf2 signaling. *Life Sci*. 2019;230:55–67. doi:10.1016/j.lfs.2019.05.056
30. Huang M, Cheng G, Tan H, et al. Capsaicin protects cortical neurons against ischemia/reperfusion injury via down-regulating NMDA receptors. *Exp Neurol*. 2017;295:66–76. doi:10.1016/j.expneurol.2017.05.001
31. Bai X, Zhu Y, Jie J, Li D, Song L, Luo J. Maackiain protects against sepsis via activating AMPK/Nrf2/HO-1 pathway. *Int Immunopharm*. 2022;108:108710. doi:10.1016/j.intimp.2022.108710
32. Sharma A, Anand SK, Singh N, Dwivedi UN, Kakkar P. AMP-activated protein kinase: an energy sensor and survival mechanism in the reinstatement of metabolic homeostasis. *Exp Cell Res*. 2023;428(1):113614. doi:10.1016/j.yexcr.2023.113614
33. Xue H, Cao H, Xing C, et al. Selenium triggers Nrf2-AMPK crosstalk to alleviate cadmium-induced autophagy in rabbit cerebrum. *Toxicology*. 2021;459:152855. doi:10.1016/j.tox.2021.152855
34. Kim Y, Kim YS, Kim HY, et al. Early Treatment with Poly(ADP-Ribose) Polymerase-1 Inhibitor (JPI-289) Reduces Infarct Volume and Improves Long-Term Behavior in an Animal Model of Ischemic Stroke. *Mol Neurobiol*. 2018;55(9):7153–7163. doi:10.1007/s12035-018-0910-6
35. Wu B, Qiu W, Wang P, et al. p53 independent induction of PUMA mediates intestinal apoptosis in response to ischaemia-reperfusion. *Gut*. 2007;56(5):645–654. doi:10.1136/gut.2006.101683
36. Qiu Z, Lei S, Zhao B, et al. NLRP3 Inflammasome Activation-Mediated Pyroptosis Aggravates Myocardial Ischemia/Reperfusion Injury in Diabetic Rats. *Oxid Med Cell Longev*. 2017;2017:9743280. doi:10.1155/2017/9743280
37. Chen L, Yan L, Zhang W. Benzoylaconine improves mitochondrial function in oxygen-glucose deprivation and reperfusion-induced cardiomyocyte injury by activation of the AMPK/PGC-1 axis. *Korean J Physiol Pha*. 2022;26(5):325–333. doi:10.4196/kjpp.2022.26.5.325
38. Ma J, Chen T, Wang R. Astragaloside IV ameliorates cognitive impairment and protects oligodendrocytes from antioxidative stress via regulation of the SIRT1/Nrf2 signaling pathway. *Neurochem Int*. 2023;167:105535. doi:10.1016/j.neuint.2023.105535
39. Wani FA, Ibrahim MA, Ameen SH, et al. Platelet Rich Plasma and Adipose-Derived Mesenchymal Stem Cells Mitigate Methotrexate-Induced Nephrotoxicity in Rat via Nrf2/Pparγ/HO-1 and NF-Kb/Keap1/Caspase-3 Signaling Pathways: oxidative Stress and Apoptosis Interplay. *Toxics*. 2023;11(5):398. doi:10.3390/toxics11050398
40. Guo K, Shang Y, Wang Z, et al. BRG1 alleviates microglial activation by promoting the KEAP1-NRF2/HO-1 signaling pathway and minimizing oxidative damage in cerebral ischemia-reperfusion. *Int Immunopharm*. 2023;119:110201. doi:10.1016/j.intimp.2023.110201
41. Paskeh MDA, Asadi A, Mirzaei S, et al. Targeting AMPK signaling in ischemic/reperfusion injury: from molecular mechanism to pharmacological interventions. *Cell Signal*. 2022;94:110323. doi:10.1016/j.cellsig.2022.110323
42. Zhu Y, Wang C, Luo J, et al. The protective role of Zingerone in a murine asthma model via activation of the AMPK/Nrf2/HO-1 pathway. *Food Funct*. 2021;12(7):3120–3131. doi:10.1039/d0fo01583k
43. Gugliandolo A, Bramanti P, Mazzon E. Activation of Nrf2 by Natural Bioactive Compounds: a Promising Approach for Stroke? *Int J Mol Sci*. 2020;21(14):4875. doi:10.3390/ijms21144875
44. Yang K, Long Q, Saja K, et al. Knockout of the ATPase inhibitory factor 1 protects the heart from pressure overload-induced cardiac hypertrophy. *Sci Rep*. 2017;7(1):10501. doi:10.1038/s41598-017-11251-8
45. Fujikawa M, Imamura H, Nakamura J, Yoshida M. Assessing actual contribution of IF1, inhibitor of mitochondrial FoF1, to ATP homeostasis, cell growth, mitochondrial morphology, and cell viability. *J Biol Chem*. 2012;287(22):18781–18787. doi:10.1074/jbc.M112.345793
46. Esparza-Moltó PB, Cuezva JM. The Role of Mitochondrial H(+)-ATP Synthase in Cancer. *Front Oncol*. 2018;8:53. doi:10.3389/fonc.2018.00053
47. Sánchez-Cenizo L, Formentini L, Aldea M, et al. Up-regulation of the ATPase inhibitory factor 1 (IF1) of the mitochondrial H+-ATP synthase in human tumors mediates the metabolic shift of cancer cells to a Warburg phenotype. *J Biol Chem*. 2010;285(33):25308–25313. doi:10.1074/jbc.M110.146480
48. Kahancová A, Sklenář F, Ježek P, Dlasková A. Regulation of glucose-stimulated insulin secretion by ATPase Inhibitory Factor 1 (IF1). *FEBS Lett*. 2018;592(6):999–1009. doi:10.1002/1873-3468.12991